

Evaluation of effective field size characteristics for small megavoltage photon beam dosimetry

H. Keivan^{1,2}, R. Maskani¹, D. Shahbazi-Gahruei^{2*}, A. Shanei², S. Pandesh³, E. Tarighati Sereshke⁴

¹School of Allied Medical Sciences, Shahroud University of Medical Sciences, Shahroud, Iran

²Department of Medical Physics, School of Medicine, Isfahan University of Medical Sciences, Isfahan, Iran

³Department of Radiology Technology, School of Allied Medicine, Birjand University of Medical Sciences, Birjand, Iran

⁴Department of Medical Physics, School of Medicine, Iran University of Medical Sciences, Tehran, Iran

ABSTRACT

► Original article

*Corresponding author:

Dr. D. Shahbazi-Gahruei

E-mail:

shahbazi@med.mui.ac.ir

Received: September 2020

Final revised: February 2021

Accepted: April 2021

Int. J. Radiat. Res., January 2022;
20(1): 163-168

DOI: 10.52547/ijrr.20.1.25

Keywords: Effective field size, small field dosimetry, ionization chamber, diode.

Background: Small photon beams are increasingly used in modern radiotherapy modalities. In small photon fields, the dosimetric field size will deviate from the nominal field size. An effective field size (FSeff) for use in small field dosimetry has been defined to overcome this issue. The present study aims to investigate the suitability of two ionization chambers and two semiconductor diodes in the measurement of 6MV photon beam profiles and to analyze the variations of FSeff in smaller fields. **Materials and Methods:** Measurements were made at 6 MV photon beams of a Siemens Artiste linear accelerator and transverse profiles were acquired for nominal square field sizes of side 1×1 to 10×10 cm² via the irradiation of detectors and radiochromic film. Full width at half maximum (FWHM) at the 50% isodose level was used to calculate FSeff. **Results:** The uncertainty of the FWHM values derived from the in-plane and cross-plane profiles (ΔFWHM%) were below 6% for all the detectors were below 6% except for Semiflex in the 1×1 field size. In small field sizes (less than 3 × 3 cm²), larger differences occurred between the dosimetric and nominal field sizes in all detectors. No significant differences between nominal and effective field sizes were observed in a field range of 4×4 - 10×10 cm². **Conclusion:** In the acquisition of small field profiles, selection of an appropriate detector is influential in accurate measurements. The findings of present study support the argument that both the size and composition of detectors affect the small field profile measurements.

INTRODUCTION

Modern techniques in radiation therapy such as image guided radiotherapy (IGRT), intensity modulated radiotherapy (IMRT), volumetric modulated arc therapy (VMAT), and stereotactic radiosurgery (SRS), and stereotactic radiotherapy (SRT), lead to the use of small therapeutic photon beams for the treatment of cancer patients ⁽¹⁾. The absence of lateral electronic equilibrium ^(2,3), source occlusion by the collimating devices, and energy spectrum changes as a function of field size ^(1,4) makes challenging in the dosimetry of small photon beams. Additionally, detector properties play a crucial role in the dosimetry accuracy ⁽¹⁾. Therefore, sophisticated dosimetric methods in small fields are necessary for the dependable determination of output factors and transverse beam profiles before the calibration of a linear accelerator (linac).

The definition of the dosimetric field size for standard fields was recommended previously by the International Electrotechnical Commission (IEC)

using Full width at half maximum (FWHM) at the 50% isodose curve in a plane perpendicular to the beam central axis at a fixed source to surface distance ⁽⁵⁾. For standard photon fields the nominal field size provides a correct representation of the dosimetric field size. In small photon fields, however, which that do not satisfy source occlusion and charged particle equilibrium, the dosimetric field size will deviate from the nominal field size, as shown by previous studies ⁽⁶⁻⁸⁾. These discrepancies impact determined output factor values and the implementation of corresponding correction factors proposed by Alfonso *et al.* in formalism for the reference dosimetry of small and non-standard fields⁽⁹⁾. In an effort to obviate these issues, Cranmer-Sargison *et al.* suggested an effective field size (FSeff) that takes into account scatter component changes and the magnitude of the dimension for small fields collimated with jaws or multileaf collimators (MLCs) ⁽⁶⁾. In this approach, a slight difference is considered between in-plane and cross-plane FWHMs.

For the sake of obtaining high precision and

accuracy, various detectors have been used in the small field dosimetry. Ionization chambers with a large sensitive volume, show uncertainties in small radiation fields owing to the volume averaging effect of a high gradient radiation field ^(10, 11). Whereas semiconductor diode detectors have relatively good radiation sensitivity and spatial resolution, they show angular dependence ⁽¹²⁾. Radiochromic films give the best spatial resolution and are tissue equivalent. Small volume ionization chambers and semiconductor diodes are usually preferred for routine measurements because they have a good signal to noise ratio and can be read out instantaneously. Moreover, they have the capability of faster measurements and repeatability ⁽¹³⁾. In some previous studies, radiochromic films or Monte Carlo simulation have been investigated in the calculation of F_{Seff} ⁽¹⁾. According our knowledge, however, F_{Seff} evaluation by detectors is not a matter to be addressed explicitly. Present work aims to examine the suitability of two small sensitive volume ionization chambers and two semiconductor diodes in the measurement of 6 MV photon beam profiles and to analyze the variations of F_{Seff} in smaller fields according to the Cranmer–Sargison approach ⁽⁶⁾.

MATERIALS AND METHODS

Experimental measurements

All exposures were performed using a 6 MV photon beam of Siemens Artiste (Siemens Medical Systems, Concord, CA, USA) linear accelerator (linac) that produces photon beams of nominal energies of 6 and 15 MV operated at a dose rates of 300 and 500 MU/min, respectively. The linac was calibrated to deliver 1 cGy/MU at a depth of maximum dose for a field size of 10×10cm² at 100cm source to surface distance.

In this study, two ionization chambers: pinpoint (PTW-Freiburg, type 31006) and Semiflex (PTW-Freiburg, type 31010) and two semiconductor detector: Diode E (PTW-Freiburg, type 60017), and diode P (PTW-Freiburg, type 60016) were used to measure small photon field lateral dose profiles. F_{Seff} was then calculated for each nominal field size. The dimensions of the detectors used in this work were provided from PTW ⁽¹⁴⁾ and are summarized in table (1).

Table 1. Main physical characteristics of the investigated detectors.

Detector	Sensitive material	Polarization voltage (V)	Sensitive volume (mm ³)	Dimensions	Package material
Semiflex (PTW-31010)	Air	300	125	5.5 mm diameter, 6.5mm length	Acrylic and graphite
Pinpoint (PTW-31016)	Air	300	16	2 mm diameter, 5 mm length	Acrylic, graphite PMMA
Diode E (PTW-60017) Unshielded	Silicon	0	0.03	1 mm ² front area 2.5 μm thickness	Epoxy resin and polymer plastic
Diode P(PTW60016) Shielded	Silicon	0	0.03	1 mm ² front area 2.5 μm thickness	Epoxy resin and metal

MP3 motorized water phantom (PTW, Freiburg, Germany) using a Tandem dual channel electrometer and a 3D scanning system, controlled by the MEPHYSTO software (PTW, Freiberg, Germany), were used for data acquisition. The positional accuracy of this water tank is 0.1mm based on the manufacture's data. Effective point of the measurement of detectors was adjusted at measurements depth using the TrueFix system (PTW-Freiburg). Detectors were oriented as recommended by the manufacturer. The pinpoint and Semiflex ionization chambers were placed with their steams perpendicular to the beam axis whereas the steams of diodes E and P were parallel. To account for dose rate fluctuations, a second Semiflex ion chamber was used as a reference detector in all fields. A bias voltage of 400 V was applied to ionization chambers while the diodes were unbiased as per manufacturer's recommendations.

Lateral dose profiles for different field settings (field sizes of 1×1 - 10×10 cm²) were obtained with the various detectors across the center of the field in cross-plane and in-plane orientations at a depth of 5

cm, sufficient to ensure the electronic build-up for the photon energy used. The acquired profiles were normalized at 100% on the central axis of the beam. The collimator jaws in y direction and MLCs in x direction collimated the radiation fields.

Film preparation and irradiation

Radiochromic films are an attractive option for the small field dosimetry, because they have high spatial resolution, are nearly water-equivalent, and do not require any processing ⁽¹⁵⁾. The radiochromic films used in this study were Gafchromic EBT3 (Ashland Inc, NJ, USA) with a sheet dimension of 20.3 × 25.4 cm². All film exposures were performed perpendicularly in polystyrene slabs of a solid water phantom. Films were handled according to the procedures outlined in the AAPM Task Group # 55 (TG-55) report ⁽¹⁶⁾. The methods proposed by Bouchard *et al.* ⁽¹⁷⁾ and Lynch *et al.* ⁽¹⁸⁾ in measurements and scanning of films were considered to decrease sources of uncertainty.

To obtain the calibration curve, a single film sheet was cut into small pieces of 4×4 cm² and irradiated

with 6 MV energy of linac at ten different monitor units (MUs) corresponding to doses ranging from 25 to 250 cGy in a fixed field size of $10 \times 10 \text{ cm}^2$ and 0° gantry. For lateral dose profile measurements of varying field sizes, film strips were positioned in the solid water phantom perpendicular to the beam. To minimize light exposure, the films were kept in black envelopes when they were not being used for scanning or irradiation.

An EPSON Expression 10000XL/PRO flatbed scanner (Seiko Epson Corp., Nagano, Japan) was used to read the transmission of the film pieces. The scanner was warmed up for at least 30 min before readings. A transparency sheet was employed to place films on the scanner in a reproducible position. In order to minimize the lateral response artifact, scans were made in the transmission mode and landscape orientation as recommended by the manufacturer. The scanner was used in 48-bit RGB (Red Green Blue) mode (16 bits per channel). Each film was read at a resolution of 150 dpi, 48 h after the irradiation, and then saved in the uncompressed tagged image file format (TIFF). The response of the radiochromic film dosimetry system is most commonly expressed as a change in the optical density between irradiated and unirradiated film pieces. The red channel was confirmed to provide higher sensitivity and was used for all analyses.

RESULTS

Lateral dose profiles and FWHM analysis

For a quantitative estimation, recorded lateral dose profiles were analyzed with MATLAB (Mathworks, Inc.) using the interpolation function. Full width half maximum (FWHM) values or the dosimetric field size were derived from the in-plane and cross-plane profiles for a range of square field sizes from 1×1 to $10 \times 10 \text{ cm}^2$. The standard deviations were $< 1.5\%$ for field sizes greater than $3 \times 3 \text{ cm}^2$ and $< 3\%$ for smaller field sizes. The uncertainty of the FWHM values for all of detectors is shown in figure 1, showing that the uncertainty of pinpoint and diode P is greater than that of diode E in all fields and the Semiflex response is large in smaller fields.

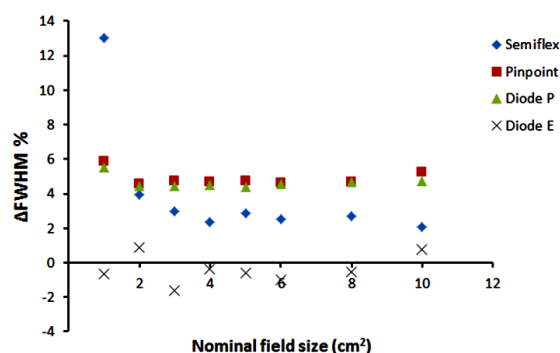


Figure 1. Percentage differences of in-plane and cross-plane FWHM derived from detector measurements in water phantom.

In general, percentage differences for the FWHM value ($\Delta\text{FWHM}\%$) were below 6% for all the detectors, except for the Semiflex in the 1×1 field size.

Percentage differences between nominal and dosimetric field sizes measured by each detector, obtained from in-plane and cross-plane profiles, are illustrated in figure 2. In field widths larger than $3 \times 3 \text{ cm}^2$, it is clear that, the responses of the Semiflex and diode E are approximately close to each other and a negligible difference is seen between them in the cross-plane profile. While all the detectors have less than 3% difference in the in-plane profile, larger difference between the dosimetric and nominal field sizes occurred in all detectors in small field sizes (less than $3 \times 3 \text{ cm}^2$). In larger field sizes, no significant difference was observed between diode E and Semiflex. It is obvious that uncertainty occurs in smaller fields in both directions.

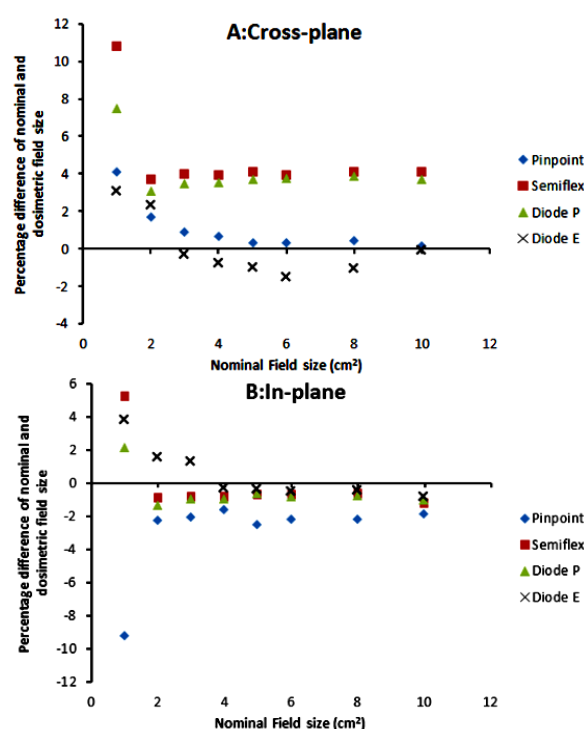


Figure 2. Percentage differences of nominal and dosimetric field sizes derived from in-plane (A) and cross-plane (B) profile data measured by detectors.

Effective field size

According to the Cranmer-Sargison approach ⁽⁶⁾, $F_{\text{Seff}} = \sqrt{A \cdot B}$, where A and B correspond to the FWHM of in-plane and cross-plane profiles. The F_{Seff} for each field size was calculated and percentage differences between nominal and effective field sizes are presented in figure 3.

Radiochromic film

Calibration curves established from the red channel were extracted from the red-green-blue scanned images. The red channel is most often used in the analysis of dose measurements because it has the highest sensitivity and absorption. The ratio of

the change in optical density and the amount of dose is illustrated in figure 4.

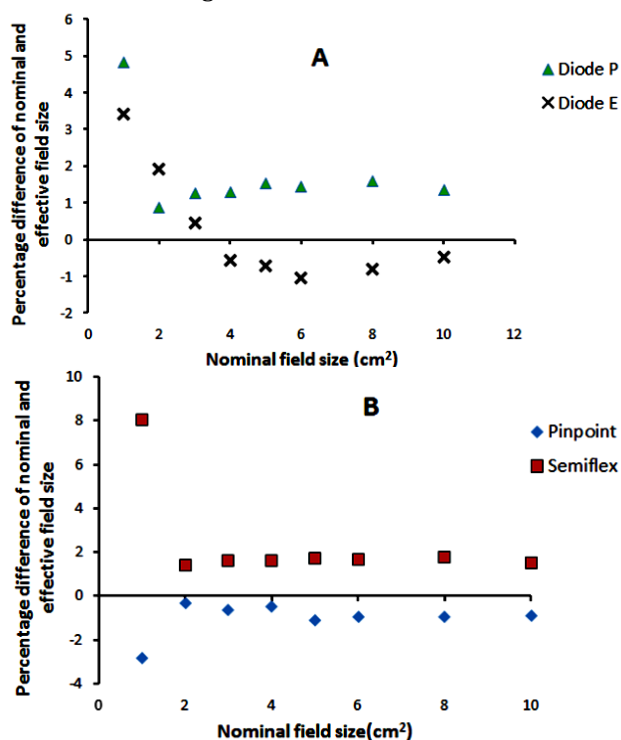


Figure 3. Percentage differences of effective and nominal field sizes derived from in-plane and cross-plane profile data. **A:** Diode P and Diode E. **B:** Pinpoint and Semiflex

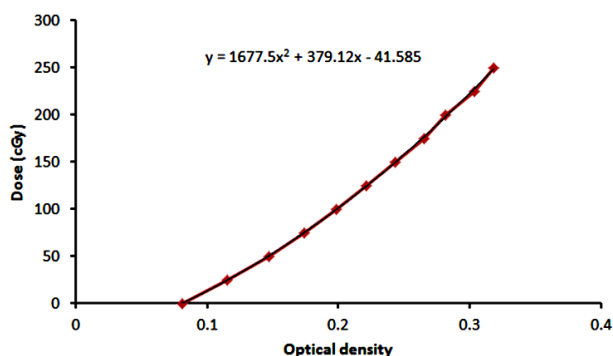


Figure 4. Calibration curve for the 6 MV photon beam with the red channel.

Since radiochromic films is almost water equivalent and considered as a detector with almost infinite resolution, doses measured from EBT3 films were employed as the reference.

For each field size, dosimetric field dimensions were determined from measurements of the FWHM derived from transversal profiles and the FSeff was calculated according to the Cranmer-Sargison ⁽⁶⁾ approach. Figure 5 shows the percentage difference between nominal and effective field sizes calculated by the film.

No significant differences are observed between nominal and effective field sizes in the field range of 4×4 - 10×10 cm². If the field size is smaller, increased variations can be seen in the percentage difference.

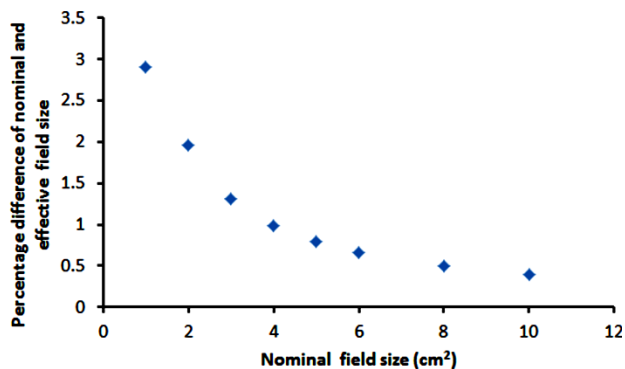


Figure 5. Percentage difference of effective and nominal field sizes derived from radiochromic film.

DISCUSSION

To characterize the FSeff in this work, FWHM values of the lateral dose profiles were determined using two diode detectors, two ionization chambers, and radiochromic film. The results of FWHM are affected by the detector properties; hence acquired the FSeff values may have uncertainty, especially in non-equilibrium small fields. Similar observations were reported in the literature ^(7,19). The difference in lateral dose profiles, measured by each detector, leads to the FWHM uncertainty. This study shows that the Semiflex behavior differs from the other detectors in smaller fields and $\Delta\text{FWHM} = 13.3\%$.

ΔFWHM values were experimentally specified in previous studies. For example, Poppinga *et al.* ⁽⁷⁾ found a 9.2% difference between in-plane and cross-plane FWHM for a 1×1 cm² field size. Biasi *et al.* ⁽²⁰⁾ found a maximum ΔFWHM value of 5.6% for the smallest field size. The uncertainty of the FWHM values in small fields for other linac models was observed by Mancosu *et al.* ⁽²¹⁾ who showed ΔFWHM values of 10.8%-15% for 0.8×0.8 cm². This difference can be attributed to the difference in calculated penumbra widths.

The differences between nominal and dosimetric field sizes for diode detectors are approximately 4%, except in the 1×1 cm² field size (figure 2). A similar study by Shin *et al.* ⁽²²⁾ using Edge diode also showed that maximum difference belonged to the smallest field size. In the 1×1 cm² field size, the average difference ratio is 4% for diode E with respect to the nominal field width in both planes, which is similar to that previously observed by Shin *et al.* ⁽²²⁾. The results of this study agree with the previous trends, for example, using a synthetic diamond detector for transverse profile measurements yielded a wider penumbra than the stereotactic field detector ⁽²³⁾.

Differences were found between the FSeff obtained with various detectors, especially in small fields (figure 3). These may be due to the influence of uncertainty on the dosimeter position relative to

other photon beam characteristics. The difference of FSeff and nominal field size has been reported in some studies. For example, Reggiori *et al.* ⁽²⁴⁾ measured nominal and effective field sizes with three detectors and showed that former systematically overestimated the effective field size for all fields up to $5 \times 5 \text{ cm}^2$. Cranmer-Sargison *et al.* ⁽²⁵⁾ used various diode detectors and concluded that this might be due to jaw calibration or their positioning inaccuracies.

Bearing in mind that film measurements are not affected by the volume averaging and detector perturbation effects, it can be assumed that the film-measured profile corresponds to the reference. The radiochromic film measurements showed that, while the FSeff were nearly identical to the nominal field sizes $\geq 1 \text{ cm}$, which confirms those done by Casar *et al.* ⁽¹⁾, who observed that they differed significantly for the field size of $1 \times 1 \text{ cm}^2$. The gafchromic film experiments demonstrated that diodes E and P exhibited similar behavior in the determination of FSeff for all field sizes, except those smaller than $1 \times 1 \text{ cm}^2$, a finding that is in agreement with that Underwood *et al.* ⁽⁸⁾. Despite the overestimate or underestimate of ionization chambers in determined dosimetric field sizes using cross-plane or in-plane profiles (figure 2), the overall results of the FSeff indicate that only the Semiflex chamber measures a very large FWHM in $1 \times 1 \text{ cm}^2$ field size. This may be due to the volume averaging effect of ionization chambers in the high gradient region, which is consistent with those reported by Sonja Wegener *et al.* ⁽¹³⁾.

Values of less than 3% for the FSeff are obtained for all the detectors in fields greater than $3 \times 3 \text{ cm}^2$ in size, which agrees with radiochromic film results. In comparison, differences greater than 4% in the FSeff are obtained for fields smaller than $3 \times 3 \text{ cm}^2$. Indeed, it was demonstrated that different detectors of the same type might have a slight difference in the dosimetric behavior.

CONCLUSION

In the acquisition of small field profiles, selection of an appropriate detector is influential in accurate measurements. The findings of the present study support the argument that both the size and composition of detectors affect the small field profile measurements. Comparisons with radiochromic film shows that a small sensitive volume ion chamber significantly overestimates the FSeff in small field sizes and accurate results in semiconductor diode yields.

ACKNOWLEDGMENT

This work is a part of PhD thesis which financially supported by Isfahan University of Medical Sciences (Grant No. 394427).

Ethical compliance: This article does not contain any studies with human participants or animals performed by any of the authors.

Conflicts of Interests: The authors declare that they have no conflicts of interest.

Funding: This work is a part of PhD thesis which financially supported by Isfahan University of Medical Sciences (Grant No. 394427).

Author contribution: Study conception and design: (H.K), (D.Sh-G), (E.T) Sereshke. Data collection: (H.K), (R.M), (S.P). Analysis and interpretation of results: (H.K), (A.Sh); Draft manuscript preparation: (D.Sh-G), (H.K), (R.M).

REFERENCES

1. Casar B, Gershkevitch E, Mendez I, Jurković S, Huq MS (2019) A novel method for the determination of field output factors and output correction factors for small static fields for six diodes and a microdiamond detector in megavoltage photon beams. *Medical physics*, **46**(2): 944-63.
2. Jafari SM, Alalawi AI, Hussein M, Alsaleh W, Najem MA, Hugtenburg RP, *et al.* (2014) Glass beads and Ge-doped optical fibres as thermoluminescence dosimeters for small field photon dosimetry. *Physics in Medicine & Biology*, **59**(22): 6875.
3. Zhu TC, editor Small field: dosimetry in electron disequilibrium region. Journal of Physics-Conference Series; 2010.
4. Tyler M, Liu PZ, Chan KW, Ralston A, McKenzie DR, Downes S, *et al.* (2013) Characterization of small-field stereotactic radiosurgery beams with modern detectors. *Physics in Medicine & Biology*, **58**(21): 7595.
5. IEC (2007) Medical Electron Accelerators-Functional Performance Characteristics.
6. Cranmer-Sargison G, Charles PH, Trapp JV, Thwaites DI (2013) A methodological approach to reporting corrected small field relative outputs. *Radiotherapy and Oncology*, **109**(3): 350-5.
7. Poppinga D, Delfs B, Meyners J, Harder D, Poppe B, Looe HK (2018) The output factor correction as function of the photon beam field size—direct measurement and calculation from the lateral dose response functions of gas-filled and solid detectors. *Zeitschrift für Medizinische Physik*, **28**(3): 224-35.
8. Underwood T, Rowland B, Ferrand R, Vieilleveigne L (2015) Application of the Exradin W1 scintillator to determine Eddiode 60017 and microDiamond 60019 correction factors for relative dosimetry within small MV and FFF fields. *Physics in Medicine & Biology*, **60**(17): 6669.
9. Lam S, Bradley D, Khandaker M (2020) Small-field radiotherapy photon beam output evaluation: detectors reviewed. *Radiation Physics and Chemistry*, **178**: 108950.
10. Alalawi AI, Jafari S, Najem M, Alsaleh W, Clark C, Nisbet A, *et al.* (2014) Preliminary investigations of two types of silica-based dosimeter for small-field radiotherapy. *Radiation Physics and Chemistry*, **104**: 139-44.
11. Keivan H, Shahbazi-Gahrouei D, Shanei A (2018) Evaluation of dosimetric characteristics of diodes and ionization chambers in small megavoltage photon field dosimetry. *Int J Radiat Res*, **16**(3): 3 11-21.
12. Araki F, Ikegami T, Ishidoya T, Kubo HD (2003) Measurements of Gamma-Knife helmet output factors using a radiophotoluminescent glass rod dosimeter and a diode detector. *Medical physics*, **30**(8): 1976-81.
13. Wegener S and Sauer OA (2018) Energy response corrections for profile measurements using a combination of different detector types. *Medical physics*, **45**(2): 898-907.
14. PTW (2019) Detectors Catalog LörracherStrae 7, 79115 Freiburg, Germany. [Available from: <http://www.ptw.de>].
15. Morales JE, Butson M, Hill R, Crowe SB, Trapp J (2020) Monte Carlo calculated output correction factors for Gafchromic EBT3 film for relative dosimetry in small stereotactic radiosurgery fields. *Physical and Engineering Sciences in Medicine*, **43**(2): 609-16.
16. Niroomand-Rad A, Blackwell CR, Coursey BM, Gall KP, Galvin JM, McLaughlin WL, *et al.* (1998) Radiochromic film dosimetry: recom-

- mendations of AAPM radiation therapy committee task group 55. *Medical physics*, **25**(11):2093-115.
17. Butson MJ, Cheung T, Yu P (2006) Scanning orientation effects on Gafchromic EBT film dosimetry. *Australasian Physics & Engineering Sciences in Medicine*, **29**(3): 281-4.
 18. Lynch BD, Kozelka J, Ranade MK, Li JG, Simon WE, Dempsey JF (2006) Important considerations for radiochromic film dosimetry with flatbed CCD scanners and EBT film. *Medical physics*, **33**(12): 4551-6.
 19. Francescon P, Kilby W, Noll J, Masi L, Satariano N, Russo S (2017) Monte Carlo simulated corrections for beam commissioning measurements with circular and MLC shaped fields on the CyberKnife M6 System: a study including diode, microchamber, point scintillator, and synthetic microdiamond detectors. *Physics in Medicine & Biology*, **62**(3): 1076.
 20. Biasi G, Petasecca M, Guatelli S, Hardcastle N, Carolan M, Pervertaylo V, et al. (2018) A novel high-resolution 2D silicon array detector for small field dosimetry with FFF photon beams. *Physica Medica*, **45**: 117-26.
 21. Mancosu P, Pasquino M, Reggiori G, Masi L, Russo S, Stasi M (2017) Dosimetric characterization of small fields using a plastic scintillator detector: a large multicenter study. *Physica Medica*, **41**: 33-8.
 22. Shin H-J, Kim M-H, Choi I-B, Kang Y-n, Kim D-H, Chio BO, et al. (2013) Evaluation of the EDGE detector in small-field dosimetry. *Journal of the Korean Physical Society*, **63**(1): 128-34.
 23. Lárraga-Gutiérrez JM, Ballesteros-Zebadúa P, Rodríguez-Ponce M, García-Garduño OA, De la Cruz OOG (2015) Properties of a commercial PTW-60019 synthetic diamond detector for the dosimetry of small radiotherapy beams. *Physics in Medicine & Biology*, **60**(2): 905.
 24. Reggiori G, Mancosu P, Suchowerska N, Lobefalo F, Stravato A, Tomatis S, et al. (2016) Characterization of a new unshielded diode for small field dosimetry under flattening filter free beams. *Physica Medica*, **32**(2): 408-13.
 25. Cranmer-Sargison G, Weston S, Sidhu NP, Thwaites DI (2011) Experimental small field 6 MV output ratio analysis for various diode detector and accelerator combinations. *Radiotherapy and Oncology*, **100**(3): 429-35.